Received: 13 August 2021 | Revised: 10 February 2022 | Accepted: 2 March 2022

DOI: 10.1002/gdj3.154

Geoscience Data Journal | RMetS | WILEY

DATA ARTICLE

Synthetic shelf sediment maps for the Greenland Sea and Barents Sea

Jack H. Laverick | **Douglas C. Speirs** | **Michael R. Heath**

Department of Mathematics and Statistics, University of Strathclyde, Glasgow, UK

Correspondence
Jack H. Laverick, Department of Mathematics and Statistics, University of Strathclyde, Glasgow G1 1XH, UK.
Email: jacklaverick@ymail.com

Funding information
Natural Environment Research Council, Grant/Award Number: NE/R012572/1

Abstract

Seabed sediment maps underpin a variety of marine research endeavours. Seabed mapping data are available for many regions, but these usually provide discrete classifications which obscure underlying continuous properties of the sediments. Other areas are poorly surveyed, e.g., polar regions which are inaccessible due to ice cover. Here, we focus on the inaccessible North East Greenland shelf for which there are almost no seabed sediment data. We trained a random forest model to predict sediment classes from an existing map of the well-surveyed neighbouring Barents Sea, using data on bathymetry, currents and waves. We then used our model to predict the unknown sediment distributions off East Greenland. In the process, we generated some new spatial data on previously un-mapped properties of the Barents Sea, such as mean grain size, organic carbon and nitrogen content, porosity and permeability. The maps of both regions are available to support future research activities in the Arctic, e.g., the parameterization of benthic biogeochemistry in ecosystem models, or mapping species distributions.

KEYWORDS

Barents Sea, grain size, Greenland Sea, seafloor, sediment maps

1 | INTRODUCTION

The Arctic is one of the most rapidly changing environments on the planet. Climate data show that the poles are warming at a faster rate than the global average (Clem, 2020; Holland & Bitz, 2003; Koenigk et al., 2020), which could result in a seasonally ice-free Arctic by the middle of the 21st century (Thackeray & Hall, 2019). Not only does temperature affect sea ice concentrations, but also biochemical processes in the ocean (Gruber, 2011) and the

Data set

Identifier: https://doi.org/10.15129/bb91fbc2-b4e9-4919-9631-bee4fb231a92

Creator: Jack Laverick, Douglas Speirs, Mike Heath

Title: Data for: Synthetic Shelf Sediment Maps for the Greenland Sea and Barents Sea

Publisher: University of Strathclyde KnowledgeBase Datasets

Publication year: 2022

Version: 1.0

composition of biological communities (Garciá Molinos, 2016), inter alia (Wassmann et al., 2011). These physical changes may soon interact with dramatic social change (Huebert, 2014). For example, the potential for an ice-free Arctic has led to questions regarding the feasibility of Arctic shipping routes (Aksenov, 2017; Ng et al., 2018). Sea ice also constrains fishing activity (Stocker et al., 2020), and although an agreement to restrict fishing in the Arctic (Hoag, 2017) has come into force, this would last for 16 years without guaranteed renewal.

These factors have motivated Arctic research programmes, including projects which would benefit from knowledge of the marine sediments of the region (e.g. MiMeMo (Heath, 2021; Heath & Daewel, 2018)). Seabed sediment data are regularly used in marine planning and modelling. Benthic organisms have specific preferences for seabed characteristics (McArthur, 2010), and so sediment maps can provide valuable inputs to habitat mapping (Robinson, 2011). The rate at which nutrient is regenerated from detritus in sediments is a major factor in the functioning of marine food webs (Nixon, 1981), and so contributes to our understanding of trophic cascades (Heath et al., 2014). Seabed sediments can act as carbon sinks (Avelar et al., 2017), so knowledge of the sedimentary environment can contribute to carbon budgets. Routine disturbance of sediments may deplete organic carbon stores (Van De Velde et al., 2018). This is especially pertinent to management plans as increased natural disturbance may result from reduced sea ice cover in shallow waters, alongside anthropogenic disturbance from activities such as bottom trawling (Martín et al., 2014).

The Greenland Sea is an Arctic ecosystem of particular interest. Sea ice in the Greenland Sea appears to block fishing activity, despite neighbouring regions in the North Atlantic supporting major fisheries (Troell et al., 2017). This sea ice is predicted to be seasonally absent by 2100 (Hofer, 2020), likely causing ecological change and opening opportunities for the exploitation of natural resources. Forecasting potential changes in the region and creating appropriate management plans is hampered by a lack of data. Details of the sediment properties of the East Greenland shelf do not exist in a spatially comprehensive and publicly available form. Recent efforts to document marine sediments off Greenland have focussed on the west coast (Jørgensbye & Wegeberg, 2018). The Danish geological survey does not provide a seabed habitat product for Greenland, and only a limited number of field samples are available in databases such as PANGAEA (pangaea.de).

In contrast to the East Greenland shelf, the sea floor sediments of the neighbouring Barents Sea are well characterized. In some ways, the Barents Sea may represent an analogue for the Greenland Sea in the future. Ice cover in the Barents Sea is less extensive (Kwok et al., 2013; Ogi et al., 2016), and anthropogenic activity levels are higher (Eguíluz et al., 2016). The Norwegian Geological Survey (NGU) in partnership with the Russian Federal State Unitarian Research and Production Company for Geological Sea Survey (SEVMORGEO) provides a spatial overview product of seafloor sediment classes in the Barents Sea (Lepland et al., 2014). NGU-SEVMORGEO defines 36 sediment classes determined by combinations of consolidated substrate, as well as proportions by weight of sediment grains binned as gravels, sands and a combination of silt and clay.

This study aims to support management and modelling activities in the Arctic by creating maps of continuous, rather than discrete, properties of sediments for the Barents Sea and the East Greenland shelf. Random forest models have already been used successfully to predict characteristics of marine sediments elsewhere (Wilson et al., 2018) by exploiting relationships between the physical environment and sediment properties. Here, we use a random forest model to predict the likely NGU-SEVMORGEO sediment classes for the Greenland Sea, assuming that the Barents Sea is a fair analogue for the region. We also take the opportunity to extend the spatial extent of the NGU-SEVMORGEO overview product to the shelf edge north of Svalbard (Figure 1). We then use the NGU-SEVMORGEO sediment classes to calculate additional variables of interest to modellers and managers, currently unavailable for either region (Table 1). Our first set of target variables are the percentages of different grain sizes and the prevalence of hard substrate. From these variables, it is possible to calculate further sediment characteristics such as mean grain size, natural disturbance rates, porosity, permeability and organic matter content (Figure 2; Wilson et al., 2018).

2 | RESULTS

2.1 | Model fit

Our model is highly accurate at reproducing Barents Sea sediment classes for our validation dataset. The balanced accuracy score within each sediment fraction was always over 90% (Figure 3) which suggests that we now have a solid basis to derive additional variables from. Predictions for rocky substrate were the most accurate at 99.6%. Predictions of silty substrate were the least accurate at 92.7%. Bed shear stress was the most important predictor of sediment class. This was followed by depth with a scaled importance of 0.82 (2 dp), while the topographic variables were largely similar in importance; roughness, TPI, TRI and slope had scaled importance of 0.51, 0.47, 0.46 and 0.45 respectively.

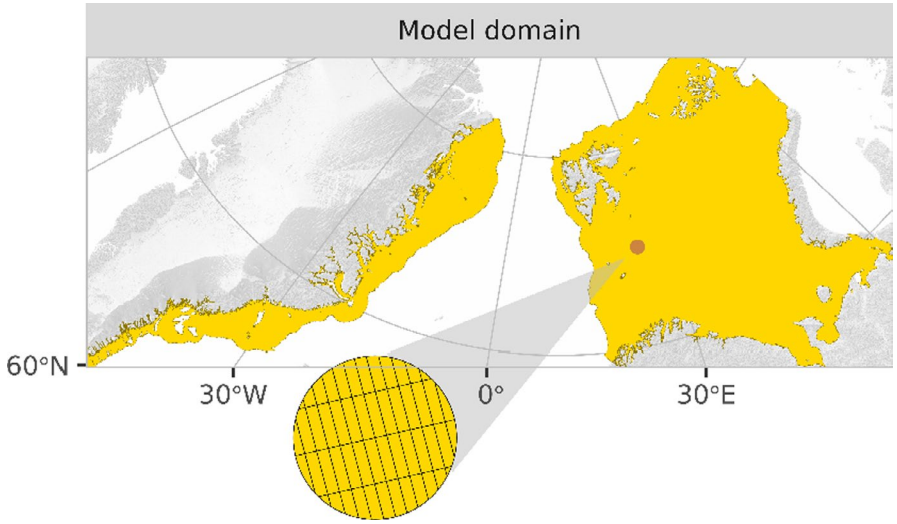

FIGURE 1 Study domain. The extent of our mapping grid is highlighted in yellow, covering the shelf area between 0 and 500 m depth in the Greenland Sea and Barents Sea. The grid has a resolution of 0.01°

TABLE 1 Data products created for a 0.01° grid. The descriptions of Roughness, TRI and TPI are quoted directly from the {raster} package documentation Hijmans and Etten (2020)

Variable	Description	Unit
Slope	Calculated according to Horn (1981).	Radians
Roughness	'The difference between the maximum and the minimum value of a cell and its 8 surrounding cells'. Hijmans and Etten (2020)	m
Terrain Ruggedness Index (TRI)	'The mean of the absolute differences between the value of a cell and the value of its 8 surrounding cells, Hijmans and Etten (2020)	m
Topographic Position Index (TPI)	'The difference between the value of a cell and the mean value of its 8 surrounding cells' (Hijmans and Etten (2020))	m
Rock	Locations with predominantly solid substrate (0 or 100).	%
Gravel, Sand, Silt	Percentage of surface sediment in each grain size class.	%
$D\bar{x}$	Mean grain size, calculated as the mean of mid-range grain sizes for each sediment fraction on a log10 scale, weighted by percent sediment fraction cover at a location.	mm
Porosity	The proportion of open space within sediment, derived from '$D\bar{x}$'.	%
Permeability	A measure of how easily water can flow through sediment, derived from 'Silt'.	m^2
Organic nitrogen content (TON)	Percentage of surface sediment as organic nitrogen by weight, derived from 'Silt'	%
Organic Carbon content (TOC)	Percentage of surface sediment as organic carbon by weight, derived from 'Silt'	%
Bed shear stress	95th percentile mean bed shear stress including waves and currents by month.	$N.m^{-2}$
Natural disturbance	Mean proportion of days in each month where the Shields stress value exceeds the critical threshold for the initiation of particle motion.	-

2.2 | Sediment fractions and mean grain size

Our results suggest that the seafloor sediments of both the Barents Sea and East Greenland shelf are predominately fine (Figure 4). The average $D\bar{x}$ for the Barents Sea was 0.226 mm to three significant figures (3sf) with a standard deviation of 0.944 mm (3sf). The sediments of the East Greenland shelf are predicted to be finer (average $D\bar{x}$ = 0.109 mm, 3sf, *SD* = 0.554 mm, 3sf). This is directly linked to the proportions of rock, gravel, sand and silt. Across the Barents Sea as a whole, the average proportions of coarse grains in seafloor sediments were higher than on the East Greenland shelf (Rock = 1.90%; *SD* = 13.6%. Gravel = 6.85%; *SD* = 14.4%. cf. Rock = 0.881%; *SD* = 9.34%. Gravel = 3.97%; *SD* = 10.1%, 3sf). The percentage of sand was comparable between the two regions at 27.8% (*SD* = 24.9%, 3sf) for the Barents Sea and 22.9% (*SD* = 17.7%, 3sf) for the East Greenland shelf. The Greenland sea had more silt at 72.2% (*SD* = 22.9%, 3sf) than the Barents Sea at 63.4% (*SD* = 30.6%, 3sf).

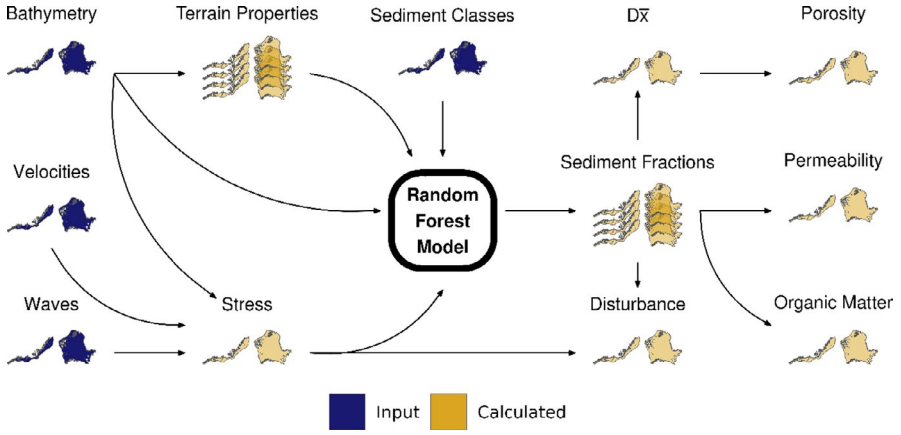

FIGURE 2 Project schematic. We predicted NGU-SEVMORGEO sediment classes (Lepland et al., 2014), using GEBCO bathymetry (GEBCO, 2019), SINMOD velocity (Slagstad & McClimans, 2005) and ECMWF wave data (Laloyaux et al., 2018) as predictors (blue). We then predicted sediment classes over a larger spatial grid, before deriving additional seafloor properties which are available with this manuscript (yellow). Arrows indicate the relationships between data products, and with our random forest model

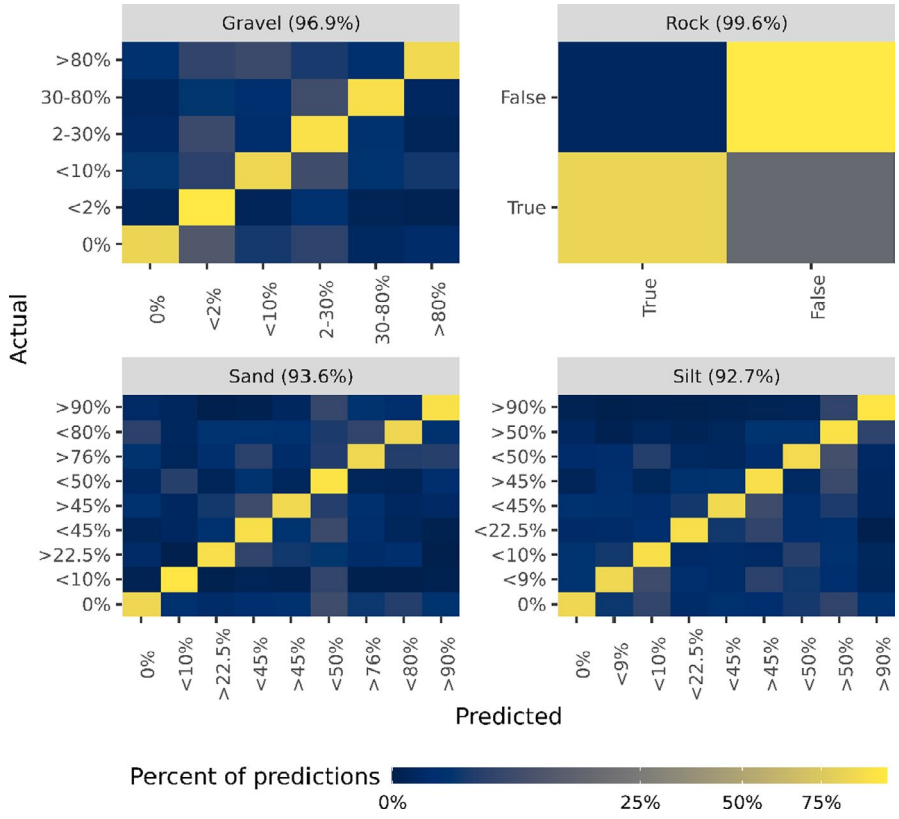

FIGURE 3 Accuracy of the random forest model for sediment classes. Each facet represents a different sediment fraction, with an absence of soft sediments defined as 'Rock'. The number in brackets in each facet label is the fraction specific balanced accuracy score. An accurate model should have high values along the diagonal, where predicted classes match actual classes. The colour scale is square root transformed to improve the visibility of small values

At smaller spatial scales, gravels can be found in the Barents Sea in shallow areas to the south of Svalbard. Sands are largely located inshore along the Russian coast, while silts are common in the north east quarter of the Barents Sea (Figure 5). For the East Greenland shelf coarse sediments are more common along the continental shelf edge to the south of our mapped area. Silts are predicted to be concentrated in cross-shelf canyons, presumably representing glacial features (Figure 5).

2.3 | Porosity and permeability

Average sediment porosity and permeability are broadly comparable between the Barents Sea (Porosity = 0.620%;

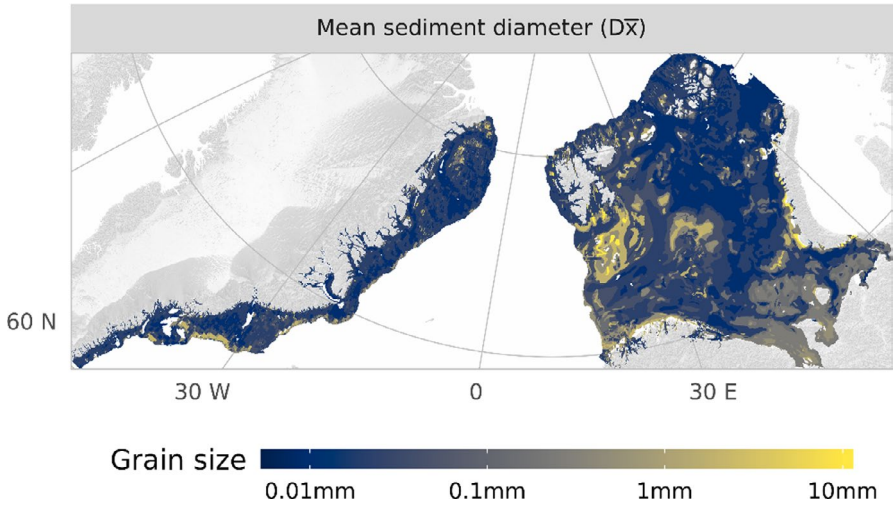

FIGURE 4 Mean sediment diameter. Sediment diameters were calculated as the mean of $\log_{10}$ transformed diameters; 11.3 mm for gravel, 0.354 mm for sand and 7.83 μm for silt (3sf), weighted by the percent composition of each sediment fraction per pixel. The data were back transformed for reporting and plotting, and can be accessed at (Laverick et al., 2022)

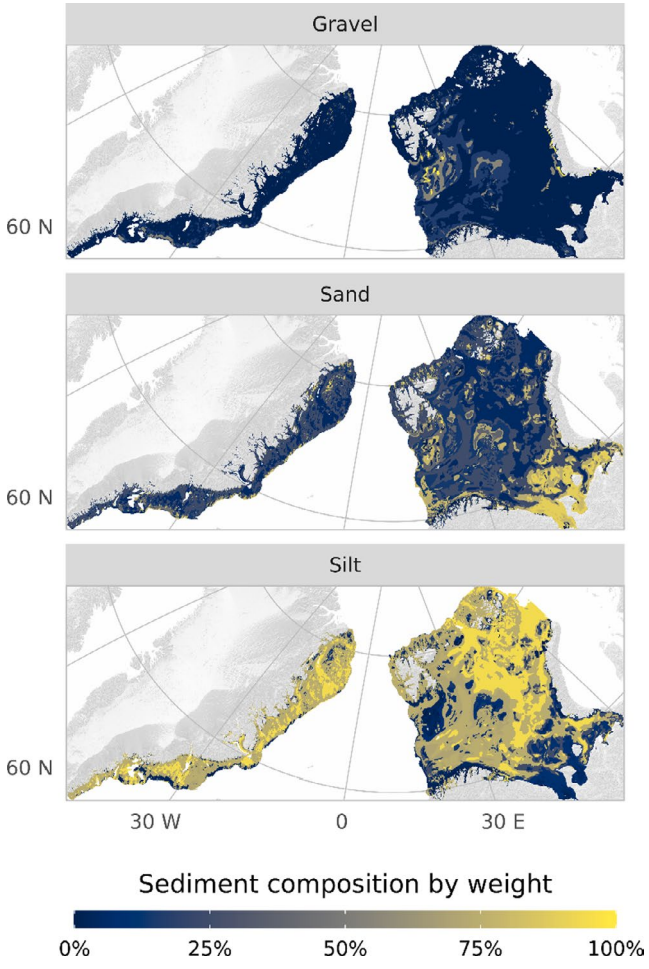

FIGURE 5 Gravel, sand and silt percentages. Sediment composition by weight of gravel (diameter 64–2 mm), sand (2 mm–62.5 μm) and silt (62.5–0.98 μm) for the Barents Sea and Greenland Sea. The maps were created by using the random forest model to predict NGU-SEVMORGEO sediment classes, and then translating classes into pseudo-continuous variables by taking the mid-values of defined ranges for each sediment fraction in a class on a $\log_{10}$ scale. The raw data to create these maps are available from (Laverick et al., 2022)

$SD = 0.114\%$; Permeability $= 6.79 \times 10^{-12}$ m^2; $SD = 4.08 \times 10^{-11}$ m^2) and East Greenland shelf (Porosity = 0.657%; SD = 0.0838%; Permeability = 2.98 x 10^{-12} m^2; $SD = 2.68 \times 10^{-11}$ m^2, 3sf). However, the Barents Sea appears to have a larger degree of spatial variability with areas of lower porosity and more permeable sediments along coastlines and to the south of Svalbard, in contrast to the rather uniform environment off Greenland (Figure 6).

2.4 | Organic matter content

Our beta regression of field sample nitrogen content against silt content returned a pseudo-R^2 of 0.6. Applying this relationship to our field of silt content resulted in a mean organic nitrogen content of 0.111% total sediment weight (SD = 0.0509%, 3sf) for the Barents Sea, and 0.109% (SD = 0.0405%, 3sf) for the East Greenland shelf. The pseudo-R^2 for organic carbon content was 0.54 with mean values of 1.17% total sediment weight (SD = 0.464%, 3sf) for the Barents Sea, and 1.28% (SD = 0.363%, 3sf) for the East Greenland shelf. The spatial patterns for both nitrogen and carbon contents are largely similar to those for silt (Figure 7) as these fields have been estimated directly from these data.

Our data validation showed that we could use the Barents Sea relationship as an analogue for the Greenland Sea. The relationships fitted for the two regions were not significantly different ($p = 0.41$ and 0.661 for N and C respectively). The Greenland dataset was limited to points inside our model domain, to avoid unrepresentative samples from the deep Fram Strait. Including all of the Greenland Data does not affect our conclusion. As a positive control, the North Sea data are best explained by a relationship significantly different to the Barents Sea relationship ($p < 1.64\ e^{-6}$ and $2\ e^{-16}$ for N and C respectively, Figure S3), where organic matter content is higher.

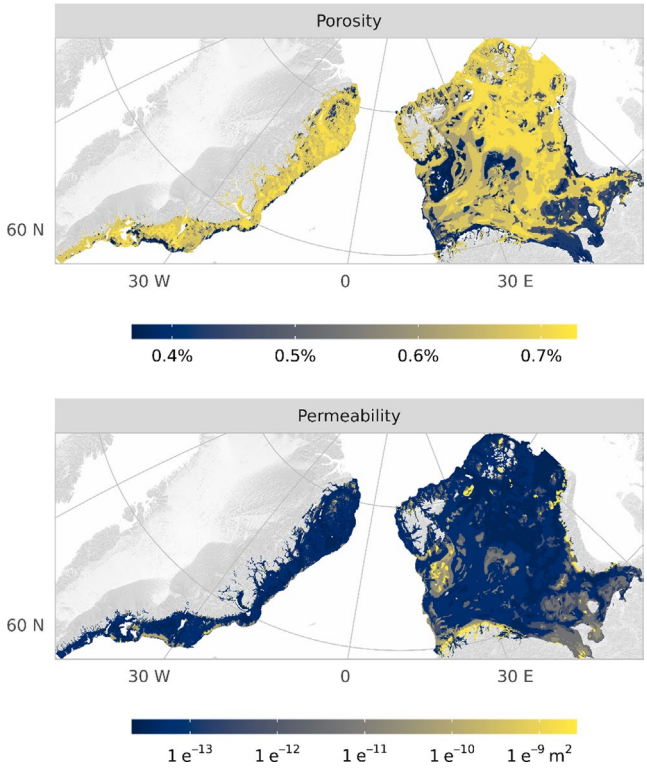

FIGURE 6 Porosity and permeability. Sediment porosity was calculated using our estimates of mean sediment diameter and the equations from (Wilson et al., 2018). Sediment permeability was calculated using our estimates of % sediment composition as silt by weight using the equations of Pace et al (Pace et al., 2021). The raw data to create these maps are available from (Laverick et al., 2022)

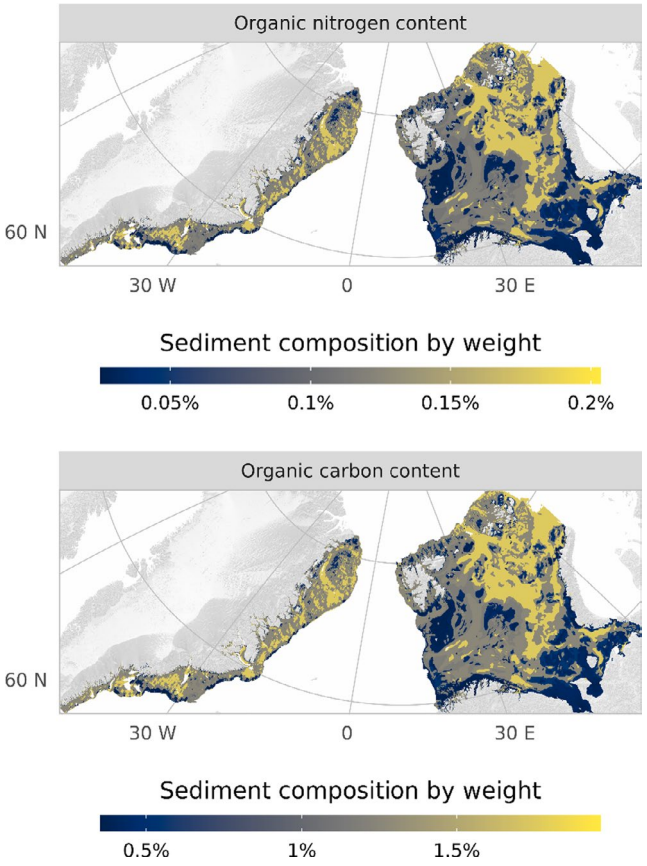

FIGURE 7 Organic matter content. Organic matter content for our mapped domain was predicted using our estimates of % sediment composition as silt by weight, and the relationship derived from (Pathirana et al., 2014). The raw data to create the map are available from (Laverick et al., 2022)

2.5 | Bed shear stress and natural disturbance

The results for bed shear stress and natural disturbance vary between the two regions. The highest bed shear stress as an average value across the entire Barents Sea is predicted to occur in September (0.116 kg.S^{-1}, SD = 0.364, 3sf). For the East Greenland shelf, this is predicted a month later in October, but is four times lower (0.0376 kg.s^{-1}, SD = 0.0571 kg.S^{-1}, 3SF). On the East Greenland shelf, this drops by approximately 25% to 0.0275 kg.S^{-1} in June (SD = 0.0396 kg.S^{-1}, 3SF). In the Barents Sea, the lowest value in the annual cycle occurs in April and is 18% lower than the peak month at 0.0950 kg.S^{-1} (SD = 0.266 kg.S^{-1}, 3SF). The spatial patterns also differ between the regions. In the Barents Sea, high bed shear stress is typically found close to shore (Figure 8), with a peak south of Svalbard in shallow water where currents can combine with wave action. In contrast, bed shear stress is highest along the continental shelf break in the East Greenland shelf and low inshore.

The low bed shear stress values mean our predictions of mean daily disturbance rate for the Greenland Sea are zero year-round. For the Barents Sea, large portions of the area are undisturbed (Figure 8). The basin-wide average is highest in August at 8.61 x 10^5% (SD = 0.00280%, 3SF) and lowest in February through April (1.17 x 10^5%, SD = 0.267%, 3SF). The areas which are disturbed coincide with shallow water to the south of Svalbard, and at the entrance to the White Sea.

3 | DISCUSSION

This study is intended to support marine research projects in the Arctic by creating extensive maps of the sediment properties of the Barents Sea and East Greenland shelf (Figure 1). To achieve this, we set out to capture the process used by NGU-SEVMORGEO to classify seabed habitats in the Barents Sea. Our results show that we can faithfully (accuracy > 90%, Figure 3) recreate the classifications produced by NGU-SEVMORGEO (NGU, 2015) using only bathymetric variables and bed shear stress data (Figure 2). Secondly, our study took the

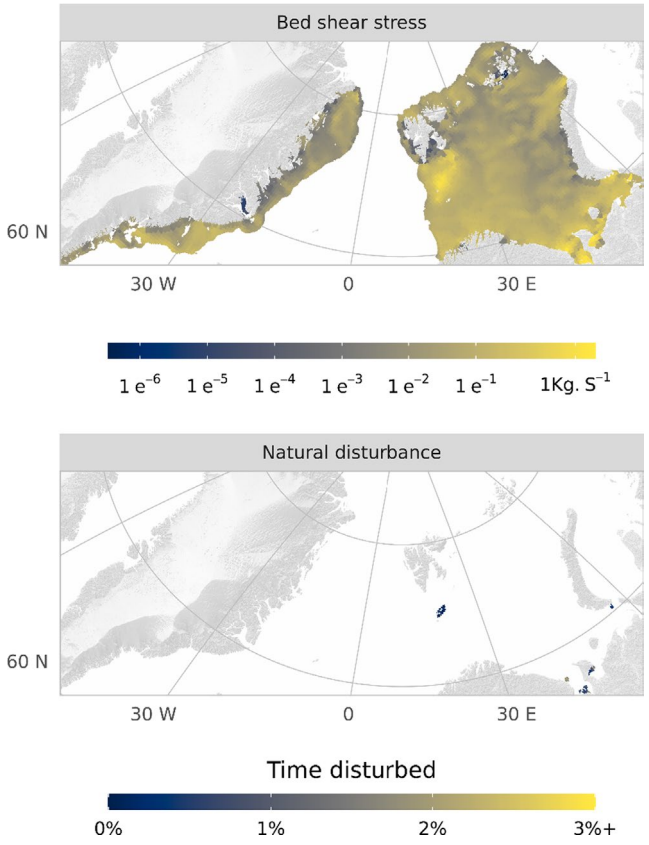

FIGURE 8 Bed shear stress and natural disturbance. Both panels display a map for the expected fields in an average October (the month with the highest natural disturbance). Both fields were calculated using the bedshear package in R (Wilson, 2019), GEBCO bathymetry (GEBCO, 2019), SINMOD velocities (Slagstad & McClimans, 2005) and EMCWF wave data (Laloyaux et al., 2018). The map of bed shear stress shows the 95th percentile of mean bed shear stress for the month, note the colour scale has been $\log_{10}$ transformed for legibility. Natural disturbance shows the mean proportion of days in a given month when the shields value exceeds the threshold for the initiation of motion. As this depends on grain size, this was calculated separately for gravel, sand and silt using 11.3 mm, 0.354 mm and 7.83 μm (3sf), respectively, and averaged weighting by the percent composition at each pixel of each sediment fraction. Areas with 0% natural disturbance have been dropped for legibility, and the colour scale has a ceiling of 3% to render low values visible. Maps of the full 12-month seasonal cycle for both variables are available in the Appendix Figure S1 and Figure S2. The data to create the maps can be accessed at (Laverick et al., 2022)

discrete habitat classes defined by NGU-SEVMORGEO and translated these into pseudo-continuous sediment variables (rock, gravel, sand, silt, Figure 5). This allowed us to calculate additional, continuous, data products which will be valuable data for future studies (Table 1, Figure 2). Finally, we used our model to predict NGU-SEVMORGEO sediment classes and calculate derived fields for the East Greenland shelf which is currently inaccessible due to persistent sea ice cover. While our results provide a modest extension to the area mapped by NGU-SEVMORGEO in the Barents Sea (Lepland et al., 2014), as well as new variables, our results for the East Greenland shelf are the most comprehensive to date (to our knowledge).

Our sediment maps are an extension of NGU-SEVMORGEO's marine sediment overview product (Lepland et al., 2014). The accuracy of our maps are dependent on the initial accuracy of these data. Further uncertainty is introduced by our translation of habitat classes into pseudo-continuous variables. By using the mid values of characteristics defining habitat types, we artificially remove extreme values. This prevents us from predicting grain sizes smaller than 7.83 μm and larger than 11.3 mm, as well as removing the variability within binned combinations of gravel, sand and silt percentages. There are similar consequences for our estimates of rock. The NGU-SEVMORGEO habitat classes do not detail the proportion of area covered by soft sediments and consolidated substrate (NGU, 2015). We, therefore, labelled habitat classes with descriptions indicating consolidated substrate as 100% rock. All other habitat classes are assumed to be 100% soft sediment. This has two consequences. We likely overestimate the proportion of the substrate comprised as rock within specific pixels labelled as rock. We likely underestimate the spatial extent of areas which contain a fraction of rock cover. We, therefore, suggest that our maps are most useful for creating zonal summaries of areas of interest for researchers; values for single pixels should be considered indicative.

Our choice to provide mean grain size on a $\log_{10}$ scale ($D\bar{x}$) instead of the more commonly used median grain size (D_{50}) also stems from the limitations imposed by translating discrete habitat classes. Grain sizes are split into classes on the Wentworth scale logarithmically (Wentworth, 1922). Calculating average grain sizes using the arithmetic mean skews estimates towards large grains like gravel, even when they are a relatively rare component of a sediment sample by weight. Using the median grain size avoids this limitation; however, as we use an indicative grain size for each of three sediment fractions, the median becomes uninformative. For a median grain size to indicate either silt or gravel in our study, it would need to comprise over 50% of the sediment by weight. In all other scenarios, the answer will be sand as the intermediate class. By calculating the arithmetic mean on $\log_{10}$ transformed values, the increments between sediment classes are linearized and the undue influence of large grain sizes removed. Using the arithmetic mean then brings the added benefit of generating values of $D\bar{x}$ other than our nominal mid-sized grain classes for each sediment fraction (Figure 4).

The most valuable addition of our study is the mapped area for the East Greenland shelf. These maps are based on the assumption that the processes shaping the Barents Sea can act as an accurate analogue of those on the east Greenland shelf. Due to its proximity, latitude and similarity as a silt dominated shelf we are of the opinion it is unlikely that there is a better analogue for the Greenland Sea than the Barents Sea. However, important differences exist. The Greenland Sea is subject to greater sea ice coverage than the Barents Sea (Ogi et al., 2016). The Barents Sea is an inflow shelf of the Arctic Ocean, receiving water from the North Atlantic, so sea ice levels are low except along its most northern shelf. The North East Greenland shelf is influenced by Arctic outflows along the East Greenland Current, which directly delivers sea ice as well as affecting temperatures. This sea ice provides an additional sediment input to the system (Masqué, 2003), when compared to the Barents Sea. This is in addition to the likely influence of glacial sediment input which is absent from the Barents Sea. High levels of sea ice in general remove the influence of surface waves from our calculations of bed shear stress, contributing to the lack of natural disturbance mapped for the East Greenland shelf. The bathymetry of the Greenland Sea also differs. For our mapped areas, the Greenland Sea is 12% deeper than the Barents Sea on average (244 m c/f 215 m, 3SF), more than twice as steep (28.1° c/f 11.8°, 3sf), and twice as rough (334 m c/f 133 m, 3sf). These differences fall within the variability of our training data, and so should be within the scope of our random forest model. There is unfortunately a lack of appropriate validation data for the East Greenland shelf, following communication with the Danish Geological Survey and searches on Pangaea.de. The interesting questions going forward are, to what extent are the sediments of the Barents Sea and Greenland Sea in a state of equilibrium? And will this be affected by melting sea ice?

4 | METHODS

4.1 | Overview

All data manipulation and modelling were conducted in the R programming language (R-Core-Team, 2019) using RStudio (RStudio-Team, 2020) and the Tidyverse (Wickham, 2019). The area of our synthetic maps covers the continental shelf of the Barents Sea and Greenland Sea at a resolution of 0.01° x 0.01° (Figure 1). The mapped extent is constrained by bathymetric contours at 0 and 500 m, and five horizontal boundaries. The mapped area for the Greenland Sea is limited by boundaries at 81.6°N and 59°N. The eastward limits to the mapped area for the Barents Sea are to the North of Severny Island (70°N, 16.23°E to 68.5°N, 20.25°E) and to the south of Yuzhny Island (68°N, 64°E to 70.74°N, 57.5°E). Our south-western limit to the Barents Sea area is along 70°N, 16.23°E to 68.5°N, 20.25° E off the Norwegian coast. These five boundaries were placed at constrictions between the two bathymetric contours. The data products produced for this grid are detailed in Table 1. The code for the analyses is available on github (https://github.com/Jack-H-Laverick/MiMeMo.Sediment).

4.2 | Model description

The Norwegian geological survey in partnership with the Russian SEVMORGEO published an overview document of seabed sediment classes in the Barents Sea (Lepland et al., 2014). We trained a random forest model, run in H2O (Aiello et al., 2018), to predict these seabed classes across our grid. Figure 2 depicts the relationships between our model, predictors and the layers we derived from our predicted seabed classes. The following subsections provide further detail on each predictor and derived field. Our model extends the existing NGU-SEVMORGEO map to the north and western shores of Svalbard, as well as to the East Greenland shelf. Training data were split 70/30 into training/validation subsets. We specified 500 trees, with other parameters left on the default settings. When assessing the accuracy of our model, we calculated balanced accuracy scores independently for each seabed fraction. This prevents a high level of accuracy in common seabed classes from masking a low level of accuracy for rare seabed classes. This also allowed our assessment to recognize the inherent similarities between the 36 sediment classes; i.e., an incorrect classification is less wrong if the two classes share some defining characteristics in terms of sediment fractions than none.

4.3 | Bathymetric variables (predictor)

Depth, slope, roughness, Terrain Ruggedness Index (TRI) and Topographic Position Index (TPI) are all used as predictors in our random forest model, as the relief of the sea floor affects sediment transport. We used the GEBCO 2019 grid as our source of bathymetry data (GEBCO, 2019), sampled on our 0.01° grid. We then used the Terrain function in the raster package (Hijmans & Etten, 2020) to calculate the other bathymetric variables at the new resolution. The derived fields are included in our supplied dataset (Laverick et al., 2022).

4.4 | Bed shear stress (predictor)

Bed shear stress also plays a major part in the distribution of marine sediments (Cheng, 2006). We calculated the 95th percentile of bed shear stress from time series at each pixel on a coarser 0.1° x 0.1° grid, using the equations from Wilson et al. (Wilson et al., 2018) available in the bedshear package (Wilson & bedshear, 2019). We used a different spatial resolution to overcome computational limits. We then used this field as a predictor for our model, joined to other explanatory variables by nearest neighbour. Calculations of bed shear stress require data on wave action and water velocities. We sourced tidally resolved water velocities for the Barents and Greenland Seas from SINMOD model outputs at 2-hr time steps (Slagstad & McClimans, 2005). Monthly mean significant wave height, wave period and wave direction data were obtained from ECMWF and CERA-20C at 3 hourly time steps (Laloyaux, 2018). The overlapping time period for the two datasets covered 2003–2010. We aligned the wave data time series with the time steps of the SINMOD velocity values by linear interpolation. The bed shear stress at a pixel in our grid was calculated using a combination of the data from the nearest neighbour on the SINMOD grid for water velocities, and from the ECMWF grid for wave data. We used a nominally small grain size of 20 μm for these calculations with depths from GEBCO as described above. We include seasonal bed shear stress in our data products associated with this manuscript (Laverick et al., 2022). The seasonal signal was calculated as the 95th percentile of bed shear stress across each calendar month over all years.

4.5 | Sediment fractions and mean grain size (derived)

NGU-SEVMORGEO defines seabed classes as combinations of different sediment fractions (NGU, 2015). We translated the Norwegian definitions for classes, recording the cover (%) for gavel, sand and silt + clay (hereafter silt). We labelled classes with predominantly hard substrate as 'Rock', with 0% cover of the three sediment fractions. Our translations are available in the Supporting Information (Appendix S1). We used the seabed classes predicted by our random forest model to create maps of hard versus soft bottom environments, as well as maps of percentage cover of each sediment fraction. As NGU-SEVMORGEO uses ranges in cover of sediment fractions and ratios between sediment fractions to define seabed classes, we used the mid-range values for each class when creating our maps. These nominal values can be found in the Supporting Information (Appendix S2).

We also create a map of mean sediment grain size ($D\bar{x}$) by calculating the average of the mid-range, on a log10 scale, diameter values for gravel (11.3 mm), sand (0.354 mm) and silt (0.00783 mm, 3sf), weighted by the cover (%) of each sediment fraction at a given location.

4.6 | Porosity and permeability (derived)

We calculated sediment porosity using our estimates of $D\bar{x}$, and the sigmoidal relationship in Wilson et al (Wilson et al., 2018). We used a different parameterization, based on additional data from samples of fine sediments (Pace et al., 2021; $p1 = -0.435$, $p2 = 0.302$, $p3 = -1.035$, $p4 = -0.314$). To predict sediment permeability across our mapped area, we used the relationship with percent sediment as silt, detailed by Pace et al. (2021).

4.7 | Organic matter content (derived)

Pathirana et al. (2014) report data on sediment fractions and organic matter content in the Barents Sea. We used beta regression for proportions to characterize the relationships between organic nitrogen and carbon content of samples with the proportion of sediment as silt or finer. We then used this model to predict organic nitrogen and carbon content across our mapped area using our random forest estimates of silt. We validated the use of the Barents Sea dataset as an analogue for the Greenland Sea by incorporating an effect of region in the beta regression and adding data from the North East Greenland Shelf (Hebbeln & Berner, 2005) and a collation of data from the North Sea (Wilson et al., 2018).

4.8 | Natural disturbance (derived)

We calculated natural disturbance as the proportion of days in a month when the Shield's value exceeded the critical threshold for the initiation of motion at each pixel in our bed shear stress grid. Both values were calculated using the bedshear package (Wilson, 2019), wave data from ECMWF and water velocities from SINMOD as outlined for our bed shear stress calculations. We used GEBCO bathymetry for depth information ([32]), and provide the data as a seasonal cycle by averaging calendar months across years. In contrast to our bed shear stress calculations, we calculated natural disturbance for each of the three sediment fractions, using a grain size of 11.3 mm for gravel, 0.354 mm for sand and 0.00783 μm for silt (3sf). We report the average of these three values, weighting by the proportion of each sediment fraction at a pixel in our grid.

ACKNOWLEDGEMENTS

This paper is from the MiMeMo project (NE/R012572/1), part of the Changing Arctic Ocean programme, jointly funded by the UKRI Natural Environment Research Council (NERC) and the German Federal Ministry of Education and Research (BMBF). We wish to thank SINTEF ocean for providing model outputs from SINMOD, and an anonymous reviewer for their constructive comments.

CONFLICT OF INTEREST

The authors declare that they have no conflict of interest.

AUTHOR CONTRIBUTIONS

Jack H. Laverick: Conceptualization (equal); Data curation (lead); Formal analysis (lead); Investigation (lead); Methodology (lead); Validation (lead); Visualization (lead); Writing – original draft (lead); Writing – review & editing (equal). **Douglas C. Speirs:** Conceptualization (equal); Funding acquisition (supporting); Methodology (supporting); Supervision (equal); Writing – original draft (supporting); Writing – review & editing (equal). **Michael R. Heath:** Conceptualization (equal); Funding acquisition (lead); Methodology (supporting); Supervision (equal); Writing – original draft (supporting); Writing – review & editing (equal).

CODE AVAILABILITY

The code for the analyses is available on github (https://github.com/Jack-H-Laverick/MiMeMo.Sediment).

DATA AVAILABILITY STATEMENT

All data products created in the course of this publication are openly available from the University of Strathclyde under 'Data for: "Synthetic Shelf Sediment Maps for the Greenland Sea and Barents Sea"'. at https://doi.org/10.15129/bb91fbc2-b4e9-4919-9631-bee4fb231a92.

OPEN PRACTICES

This article has earned an Open Data badge for making publicly available the digitally shareable data necessary to reproduce the reported results. The data is available at https://doi.pangaea.de/10.1594/PANGAEA.936921. Learn more about the Open Practices badges from the Center for Open Science: https://osf.io/tvyxz/wiki.

ORCID

Jack H. Laverick https://orcid.org/0000-0001-8829-2084

REFERENCES

Aiello, S., Eckstrand, E., Fu, A., Landry, M. & Aboyoun, P. (2018) Machine Learning with R and H2O. CA USA; http://h2o.ai/resources/

Aksenov, Y., Popova, E.E., Andrew Yool, A.J., Nurser, G., Williams, T.D., Bertino, L. et al. (2017) On the future navigability of Arctic sea routes: high-resolution projections of the Arctic Ocean and sea ice. *Marine Policy*, 75, 300–317.

Avelar, S., van der Voort, T.S. & Eglinton, T.I. (2017) Relevance of carbon stocks of marine sediments for national greenhouse gas inventories of maritime nations. *Carbon Balance and Managment*, 12, 10.

Cheng, N.S. (2006) Influence of shear stress fluctuation on bed particle mobility. *Physics of Fluids*, 18, 96602.

Clem, K.R., Fogt, R.L., Turner, J., Lintner, B.R., Marshall, G.J., Miller, J.R. et al. (2020) Record warming at the South Pole during the past three decades. *Nature Climate Change*, 10, 762–770.

Eguíluz, V.M., Fernández-Gracia, J., Irigoien, X. & Duarte, C.M. (2016) A quantitative assessment of Arctic shipping in 2010–2014. *Scientific Reports*, 6, 1–6.

GEBCO Bathymetric Compilation Group (2019) The GEBCO_2019 Grid - a continuous terrain model of the global oceans and land. British Oceanographic Data Centre, National Oceanography Centre, NERC, UK.

Gruber, N. (2011) Warming up, turning sour, losing breath: Ocean biogeochemistry under global change. *Philosophical Transactions of the Royal Society A: Mathematical, Physical and Engineering Sciences*, 369, 1980–1996.

Heath, M.R., Benkort, D., Brierley, A.S., Daewel, U., Laverick, J.H., Proud, R. et al. (2021) Ecosystem approach to harvesting in the Arctic: Walking the tightrope between exploitation and conservation in the Barents Sea. *Ambio*, 51(2), 1–15. https://doi.org/10.1007/S13280-021-01616-9/TABLES/2

Heath, M.R., Cook, R.M., Cameron, A.I., Morris, D.J. & Speirs, D.C. (2014) Cascading ecological effects of eliminating fishery discards. *Nature Communications*, 5, 1–8.

Heath, M.R. & Daewel, U. (2018) *MiMeMo - Changing Arctic Ocean*. Available at: https://www.changing-arctic-ocean.ac.uk/project/mimemo/ [Accessed: 23rd March 2021].

Hebbeln, D. & Berner, H. (2005) Bulk sediment parameter measured on surface sediment samples of Sites PS1230-1 to PS15/060. PANGAEA. https://doi.org/10.1594/PANGAEA.56575

Hijmans, R.J. & van Etten, J. (2020) Geographic data analysis and modeling [R package raster]. http://CRAN.R-project.org/package=raster

Hoag, H. (2017) Nations agree to ban fishing in Arctic Ocean for at least 16 years. *Science*. https://doi.org/10.1126/science.aar6437

Hofer, S., Lang, C., Amory, C., Kittel, C., Delhasse, A., Tedstone, A. et al. (2020) Greater Greenland Ice Sheet contribution to global sea level rise in CMIP6. *Nature Communications*, 11, 1–11.

Holland, M.M. & Bitz, C.M. (2003) Polar amplification of climate change in coupled models. *Climate Dynamics*, 21, 221–232.

Horn, B.K.P. (1981) Hill shading and the reflectance map. *Proceedings of the IEEE*, 69, 14–47.

Huebert, R. (2014) Rising temperatures, rising tensions: Power politics and regime building in the Arctic. In *Polar oceans governance in an era of environmental change*. Edward Elgar Publishing Ltd., pp. 65–85. https://doi.org/10.4337/9781781955451.00013

Jørgensbye, H. & Wegeberg, S. (2018) Mapping of marine sediments on the Greenland West Coast: contributions of fishers' ecological knowledge. *ICES Journal of Marine Science*, 75, 1768–1778.

Koenigk, T., Key, J., & Vihma, T. (2020) Climate change in the Arctic. In A. Kokhanovsky & C. Tomasi (Eds.), *Physics and chemistry of the arctic atmosphere*. Cham: Springer, pp. 673–705. https://doi.org/10.1007/978-3-030-33566-3_11

Kwok, R., Spreen, G. & Pang, S. (2013) Arctic sea ice circulation and drift speed: decadal trends and ocean currents. *Journal of Geophysical Research Ocean*, 118, 2408–2425.

Laloyaux, P., de Boisseson, E., Balmaseda, M., Bidlot, J.-R., Broennimann, S., Buizza, R. et al. (2018) CERA-20C: a coupled reanalysis of the twentieth century. *Journal of Advances in Modeling Earth Systems*, 10, 1172–1195.

Laverick, J.H., Speirs, D.C. & Heath, M.R. (2022) Data for: 'synthetic shelf sediment maps for the Greenland Sea and Barents Sea'. PURE, https://doi.org/10.15129/bb91fbc2-b4e9-4919-9631-bee4fb231a92

Lepland, A., Rybalko, A. & Lepland, A. (2014) Seabed Sediments of the Barents Sea. Scale 1:3 000 000. Trondheim & St. Petersburg: Geological Survey of Norway & SEVMORGEO. https://kartkatalog.geonorge.no/metadata/norges-geologiske-undersokelse/bunnsedimenter-kornstorrelse-oversikt/39c357fc-8c56-49e0-a6ba-3e434d62a585

Martín, J., Puig, P., Palanques, A. & Giamportone, A. (2014) Commercial bottom trawling as a driver of sediment dynamics and deep seascape evolution in the Anthropocene. *Anthropocene*, 7, 1–15.

Masqué, P., Cochran, J.K., Hebbeln, D., Hirschberg, D.J., Dethleff, D. & Winkler, A. (2003) The role of sea ice in the fate of contaminants in the Arctic Ocean: plutonium atom ratios in the fram strait. *Environmental Science and Technology*, 37, 4848–4854.

McArthur, M.A., Brooke, B.P., Przeslawski, R., Ryan, D.A., Lucieer, V.L., Nichol, S. et al. (2010) On the use of abiotic surrogates to describe marine benthic biodiversity. *Estuarine, Coastal and Shelf Science*, 88, 21–32.

Molinos, J.G., Halpern, B.S., Schoeman, D.S., Brown, C.J., Kiessling, W., Moore, P.J. et al. (2016) Climate velocity and the future global redistribution of marine biodiversity. *Nature Climate Change*, 6, 83–88.

Ng, A.K.Y., Andrews, J., Babb, D., Lin, Y. & Becker, A. (2018) Implications of climate change for shipping: opening the Arctic seas. *Wiley Interdisciplinary Reviews: Climate Change*, 9, e507.

NGU (2015) NGU. SOSI Produktspesifikasjon versjon, 4.0 - 2 - Produktnavn: ND_Bunnsedimenter_kornstørrelse, versjon. City Trondheim: Institution Geological Survey of Norway. https://www.ngu.no/upload/Kartkatalog/Produktspesifikasjon_Marin_SedimentKornstorrelse.pdf

Nixon, S.W. (1981) Remineralization and nutrient cycling in coastal marine ecosystems. In: Neilson, B.J. & Cronin, L.E. (Eds.) *Estuaries and nutrients*. Humana Press, pp. 111–138. https://doi.org/10.1007/978-1-4612-5826-1_6

Ogi, M., Rysgaard, S. & Barber, D.G. (2016) The influence of winter and summer atmospheric circulation on the variability of temperature and sea ice around Greenland. *Tellus Series A: Dynamic Meteorology and Oceanography*, 68, 31971.

Pace, M.C., Bailey, D.M., Donnan, D.W., Narayanaswamy, B.E., Smith, H.J., Speirs, D.C. et al. (2021) Modelling seabed sediment physical properties and organic matter content in the Firth of Clyde. *Earth System Science Data*, 13, 5847–5866.

Pathirana, I., Knies, J., Felix, M. & Mann, U. (2014) Sand fraction, organic carbon and nitrogen data, and calculated marine and terrestrial organic carbon fractions of surface sediments in the western Barents Sea. Pangaea, https://doi.org/10.1594/PANGAEA.817232

R-Core-Team (2019) *A language and environment for statistical computing*. Vienna, Austria: R Foundation for Statistical Computing. http://www.r-project.org/

Robinson, K.A., Ramsay, K., Lindenbaum, C., Frost, N., Moore, J., Wright, A.P. et al. (2011) Predicting the distribution of seabed biotopes in the southern Irish Sea. *Continental Shelf Research*, 31, S120–S131.

RStudio-Team, (2020) *RStudio: Integrated Development for R*.

Slagstad, D. & McClimans, T.A. (2005) Modeling the ecosystem dynamics of the Barents sea including the marginal ice zone: I. Physical and chemical oceanography. *Journal of Marine Systems*, 58, 1–18.

Stocker, A.N., Renner, A.H.H. & Knol-Kauffman, M. (2020) Sea ice variability and maritime activity around Svalbard in the period 2012–2019. *Scientific Reports*, 10, 1–12.

Thackeray, C.W. & Hall, A. (2019) An emergent constraint on future Arctic sea-ice albedo feedback. *Nature Climate Change*, 9, 972–978.

Troell, M., Eide, A., Isaksen, J., Hermansen, Ø. & Crépin, A.S. (2017) Seafood from a changing Arctic. *Ambio*, 46, 368–386.

Van De Velde, S., Van Lancker, V., Hidalgo-Martinez, S., Berelson, W.M. & Meysman, F.J.R. (2018) Anthropogenic disturbance keeps the coastal seafloor biogeochemistry in a transient state. *Scientific Reports*, 8, 1–10.

Wassmann, P., Duarte, C.M., Agustí, S. & Sejr, M.K. (2011) Footprints of climate change in the Arctic marine ecosystem. *Global Change Biology*, 17, 1235–1249.

Wentworth, C.K. (1922) A scale of grade and class terms for clastic sediments. *The Journal of Geology*, 30, 377–392.

Wickham, H., Averick, M., Bryan, J., Chang, W., McGowan, L.D., François, R. et al. (2019) Welcome to the Tidyverse. *Journal of Open Source Software*, 4, 1686.

Wilson, R.J. (2019) bedshear [R package]. https://github.com/r4ecology/bedshear#readme

Wilson, R.J., Speirs, D.C., Sabatino, A. & Heath, M.R. (2018) A synthetic map of the north-west European Shelf sedimentary environment for applications in marine science. *Earth System Science Data*, 10, 109–130.

SUPPORTING INFORMATION

Additional supporting information may be found in the online version of the article at the publisher's website.

How to cite this article: Laverick, J.H., Speirs, D.C. & Heath, M.R. (2022) Synthetic shelf sediment maps for the Greenland Sea and Barents Sea. *Geoscience Data Journal*, 00, 1–11. Available from: https://doi.org/10.1002/gdj3.154